Cell Reports, Volume *45*

Supplemental information

Mechanisms of premotor-motor cortex interactions during movement initiation

Mansour Alyahyay, Julian J. Ammer, Gabriel Kalweit, Hao Zhu, Ahmed Adzemovic, Maria Kalweit, Golan Karvat, Artur Schneider, Yixin Tong, Mate D. Döbrössy, Zoe Jäckel, Cemal Akmese, Andreas Vlachos, Joschka Boedecker, and Ilka Diester

Supplemental Information

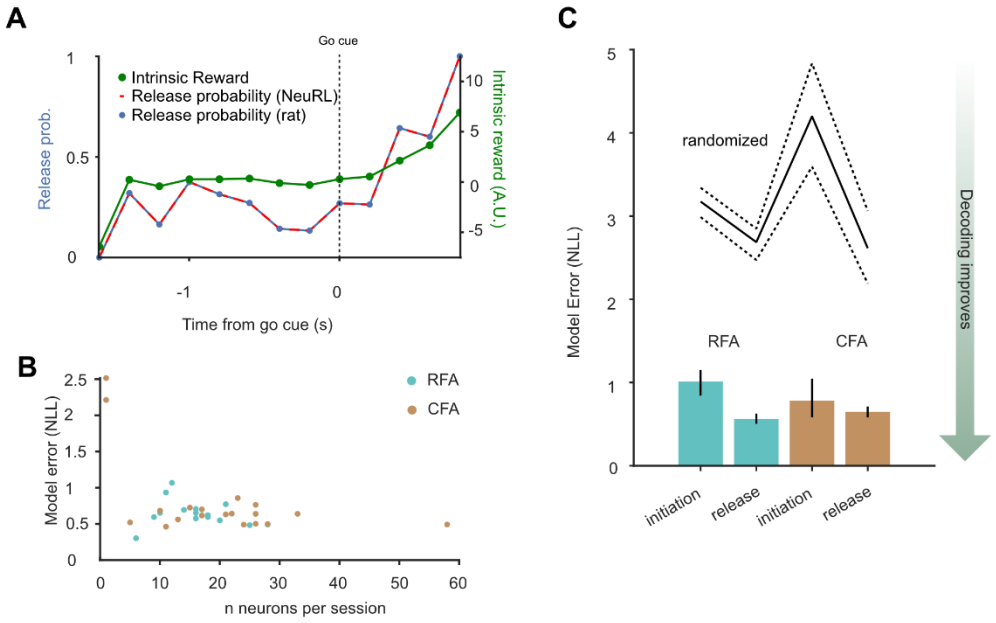


Figure S1. NeuRL decoding, related to Figure1.

(A) Learned intrinsic reward (green) and the resulting performance as probability of release for each time bin (red dashed line) plotted with the actual release probability of one example rat (blue).

(B) Model error for the decoding of lever release with NeuRL in RFA and CFA (N = 5 rats) for all sessions as a function of number of neurons per session.

(C) Decoding of task initiation and lever release with NeuRL in RFA and CFA (N = 5 rats). The model error for decoding the release time via NeuRL was quantified as negative log likelihood (NLL). Error bars depict 95% confidence intervals.

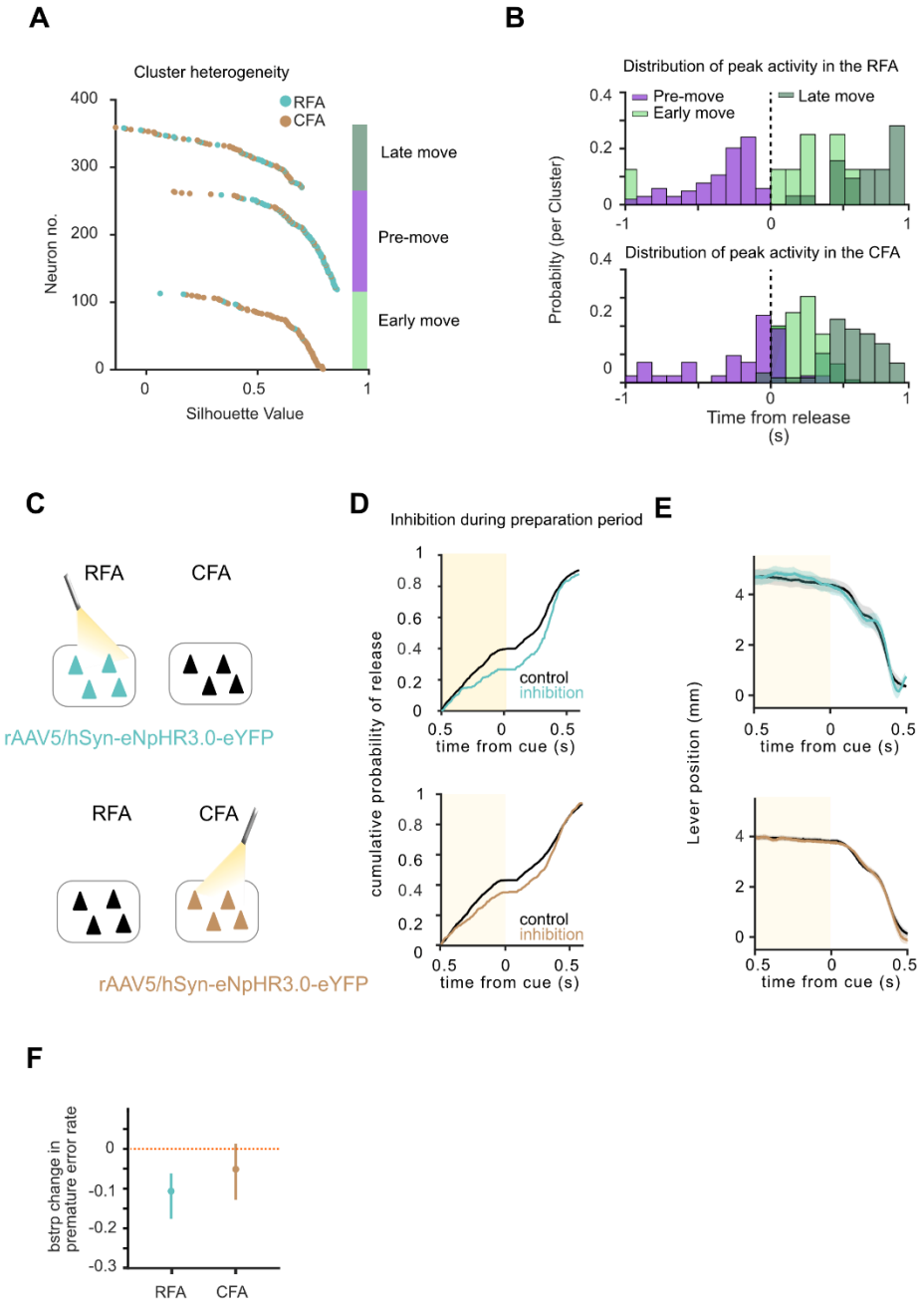


Figure S2. Cluster heterogeneity and effect of individual optogenetic inhibition of RFA or CFA, related to Figure 2.

(A) Silhouette plots illustrating the heterogeneity in the k-means clusters. Closed circles, individual units.

(B) Probability distribution of peak activity times normalized for each cluster for RFA (top) and CFA (bottom). Note that despite the heterogeneity within clusters, neurons are split into clusters with predominantly pre-movement, early movement and late movement neurons.

(C) Top: Schematic of optogenetic manipulation in RFA, rAAV5/hSyn-eNpHR3.0-eYFP was injected into RFA and a fiber implanted. Bottom: Optogenetic manipulation in CFA.

(D) Top: Average cumulative release time (N = 3 rats, n = 15 sessions) in response to 0.5 s inhibition in RFA prior to the cue in blue. Control condition in black. Bottom: Inhibition in CFA (N = 4 rats, n = 23 sessions) in brown.
(E) Top: Average lever trajectories in correct trials (N = 3 rats, n = 15 sessions) in response to 0.5 s inhibition in RFA prior to the cue in blue. Control condition in black. Bottom: Inhibition in CFA (N = 4 rats, n = 23 sessions) in brown. Note that there is no effect of optogenetic inhibition on lever position during the preparation phase.
(F) Median bootstrapped change in premature error rate with 95% confidence interval for RFA (blue) and CFA (brown), dashed line indicates 0 change, n = 1000 bootstraps with mean of n = 15 sessions each.

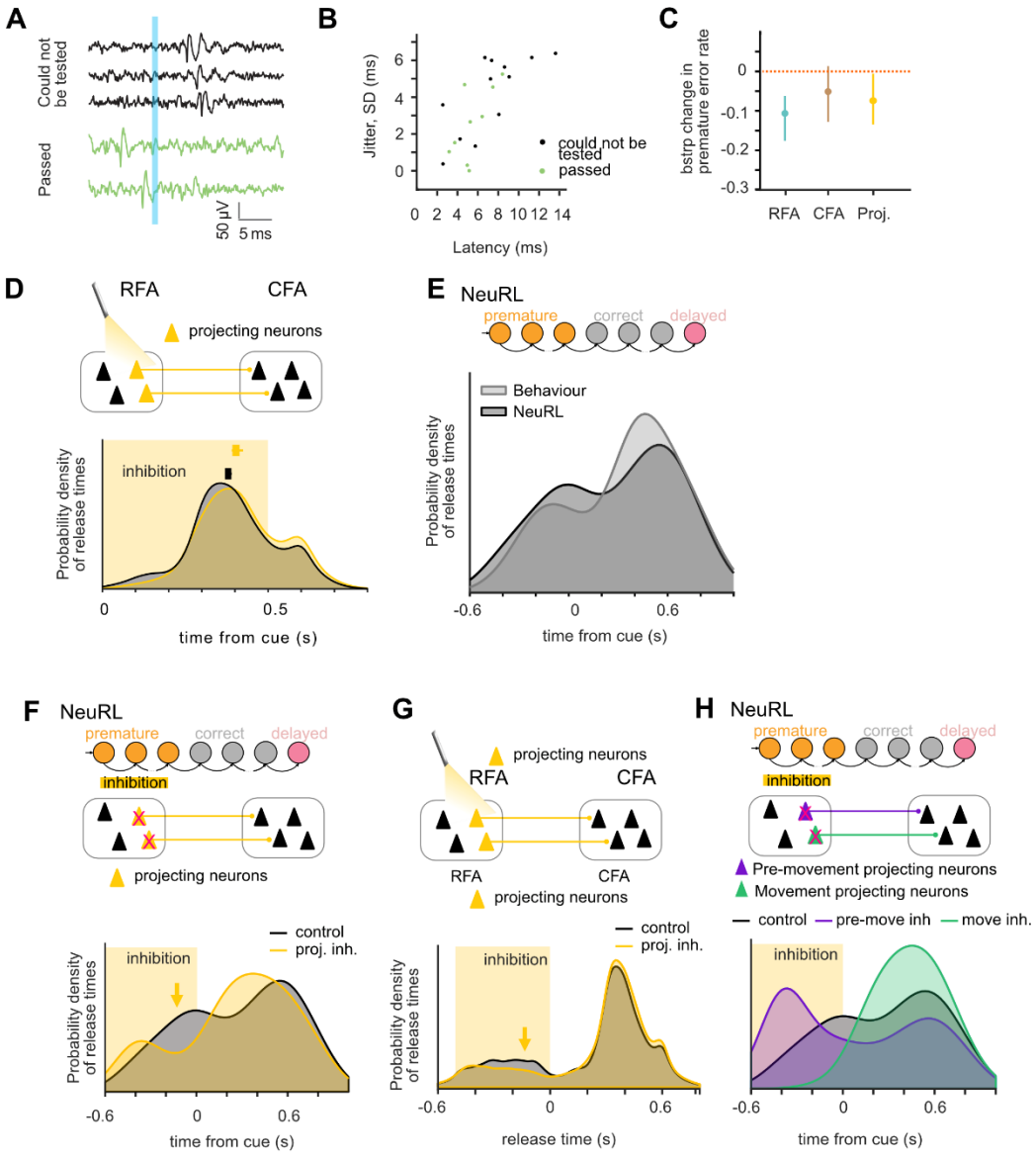


Figure S3. Spontaneous collision test and behavioral predictions by NeuRL, related to Figure 3.
(A) Example traces for photo-triggered spikes without (black) and with (green) preceding spontaneous action potential.
(B) Scatter plot of spike timing jitter and spike latency of first spike after laser onset. Green dots refer to units that passed the collision test, i.e. a spontaneously occurring spike before the optogenetic stimulation pulse prevented the backpropagation or generation of an antidromic spike. Black dots refer to units which could not be tested due to the absence of spontaneously occurring spikes preceding the laser pulse.
(C) Median bootstrapped change in premature error rate with 95% confidence interval for RFA (blue), CFA (brown) and RFA to CFA projecting neurons (yellow) dashed line indicates 0 change, n = 1000 bootstraps with mean of n = 15 sessions each. Data are replotted from Fig S2G and Fig 3I.
(D) Top: Schematics for inhibition of neurons projecting from RFA to CFA. Bottom: Probability density of release times in control (black) and after inhibition (yellow) during the movement period relative to cue onset (N = 4 rats with n = 32 sessions).

(E) Probability density of release times in control behaviour (black, N=3 rats), and for the NeuRL model (gray). Behavioural data was binned in 200ms bins for a direct comparison with NeuRL.
(F) Top: Schematics for *in silico* inhibition of putative RFA to CFA projecting neurons. We inhibited RFA to CFA-projecting neurons during the pre-movement period (N = 3 rats, 1,000 simulations for each rat), using NeuRL. Bottom: Probability density of release times for control (black) and inhibition of projecting neurons (yellow). Note that NeuRL was trained on neural activity recorded in a first cohort subjected to electrophysiology only, whereas optogenetic experiments were performed in a second cohort without electrophysiological recording (Fig 3 H). Note, that the model also predicts a leftward shift in the peak of the release time distribution following the cue which we did not observe in the optogenetic experiments in E.
(G) Top: Schematics for inhibition of neurons projecting from RFA to CFA. Bottom: Probability density of release times in control (black) and after inhibition (yellow) during the preparation period (N = 4 rats with n = 32 sessions).
(H) Schematics for *in silico* inhibition of subpopulations of putative RFA to CFA projecting neurons. Probability density of release times in control (black), and when inhibiting the pre-movement subpopulation (purple) or movement subpopulation (green) during the preparation period.

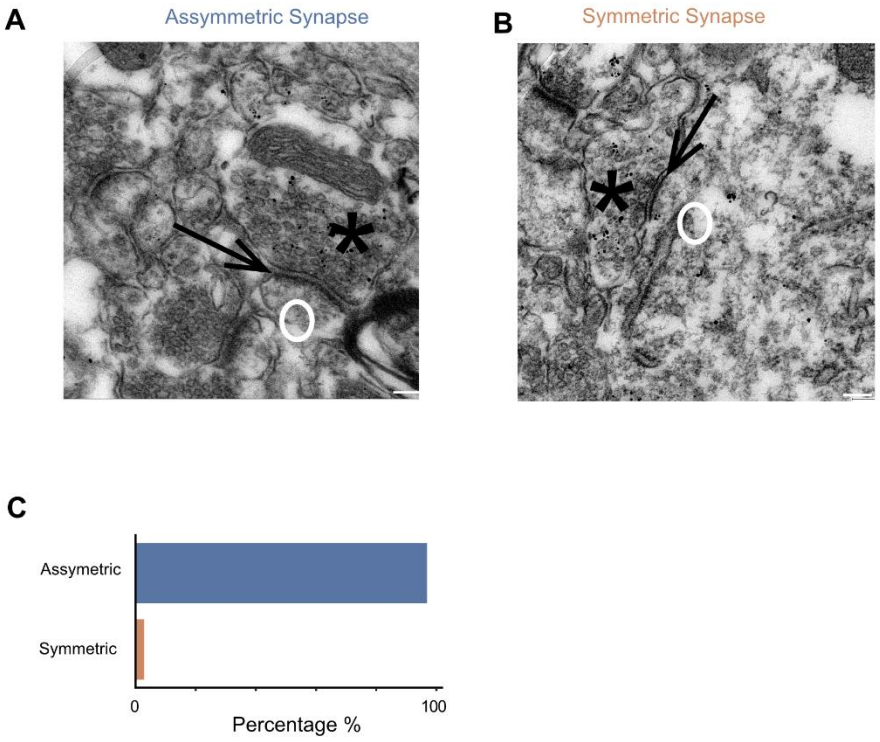


Figure S4. Asymmetry of synapses, related to Figure 4.
(A) EM image showing an asymmetric synapse. Asterisk: presynapse, circle: post synapse, arrow: synaptic cleft. Note the thick post synaptic density.
(B) Same as A for symmetric synapse.
(C) Percentage of asymmetric and symmetric synapses.

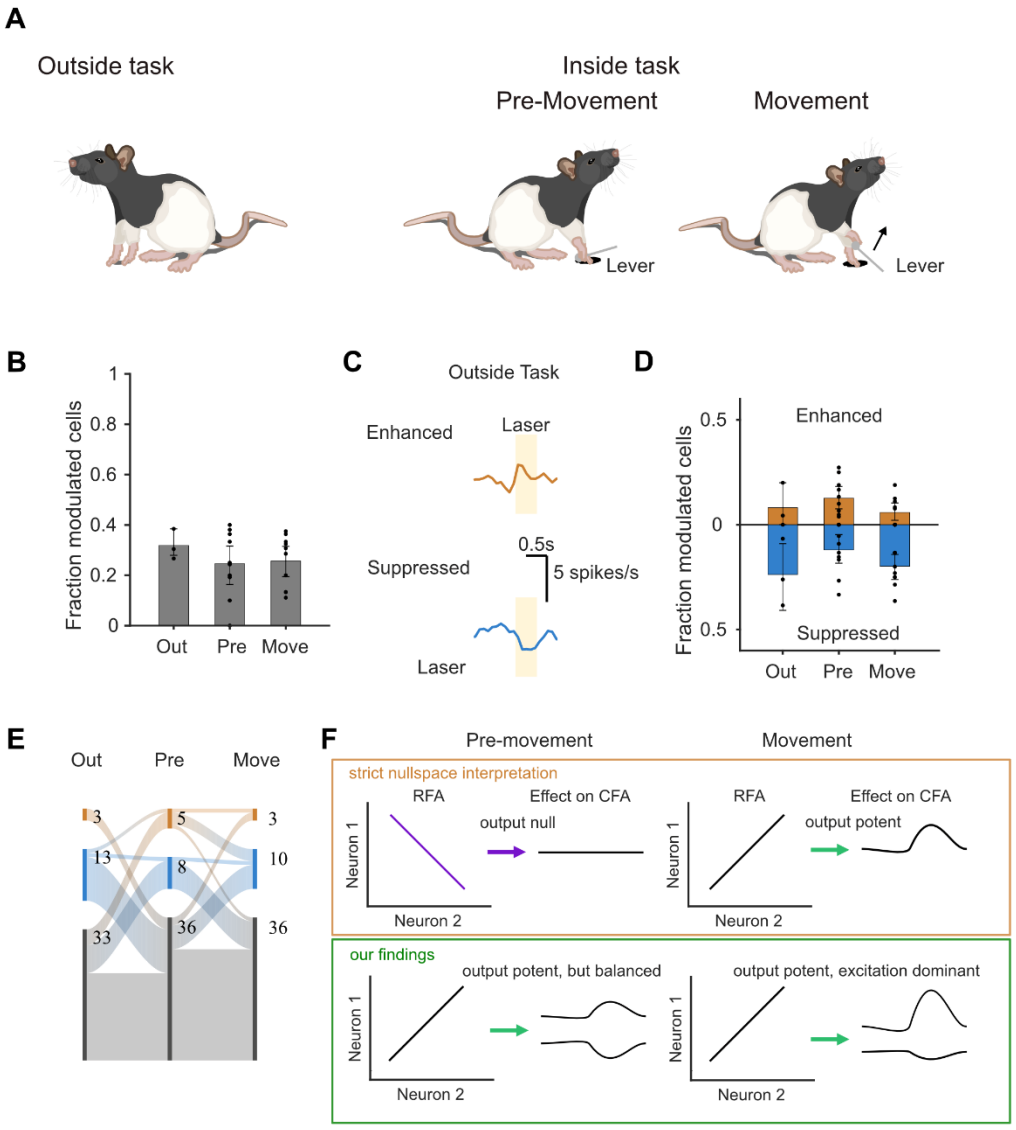


Figure S5. CFA responses to RFA input modulation outside the task, during pre-movement and during movement, related to Figure 5.

(A) Schematic of the investigated behavioral epochs. Optogenetic experiments were performed either outside the task, during the preparation period, or the movement period.

(B) Fractions of modulated cells, single dots refer to individual sessions. Error bars depict 95% confidence intervals.

(C) Average of enhanced and suppressed neuron populations when silencing RFA outside the task.

(D) Fraction of enhanced and suppressed cells across task states. Error bars depict 95% confidence intervals.

(E) Sankey plot illustrating the reorganization of CFA neurons influenced by RFA input. Distinct populations are affected outside the task and during preparation.

(F) Simplified schematic of possible communication schemes between RFA and CFA during pre-movement (left) and movement (right). Please note that output potent does not necessarily mean movement potent.

Rat #	Recording area	Injection coordinates		
		AP (mm)	ML (mm)	DV of shank tip (mm)
10	RFA	+3.8	-1.7	2.4
12	RFA	+3.7	-1.5	2.4
504	RFA	+3.2	-1.9	2.4
533	RFA	+3.5	-2.0	2.4
546	RFA	+3.5	-2.0	2.4
1	CFA	+0.2	-2.2	2.4
3	CFA	+0.6	-2.5	2.4
13	CFA	-0.1	-2.1	2.4
16	CFA	+0.3	-2.8	2.4
506	CFA	-0.5	-2.4	2.4

Table S1: Coordinates of silicon probe implantation sites in the RFA and CFA. Related to Figure 1.

Rat #	Injection area	Viral vector	Injection coordinates			Laser area	Recording area
			AP (mm)	ML (mm)	DV of shank tip (mm)		
10	RFA	AAV-hSyn-ChR2	+3.5	-1.5	2.4	CFA	RFA
12	RFA	AAV-hSyn-ChR2	+3.4	-1.6	2.4	CFA	RFA
546	RFA	AAV-hSyn-ChR2	+3.5	-1.5	2.4	CFA	RFA

Table S2: Injection coordinates in photo-tagging experiments. Related to Figure 3.

Rat #	Injection area	Viral vector	Coordinates left (mm)			coordinates right (mm)			Laser area	Recording area
			AP	ML	DV	AP	ML	DV		
3	RFA	AAV-DIO-eNpHr	3.7	1.5	0.6/1.2	3.6	1.7	0.6/1.2	RFA	CFA
	CFA	retroAAV-cre	0.5/0.0	2.2/2.3	0.6/1.2	0.7/0.1	2.5/2.5	0.6/1.2		
13	RFA	AAV-DIO-eNpHr	3.8	3.5	0.6/1.2	3.5	1.5	0.6/1.2	RFA	CFA
	CFA	retroAAV-cre	0.37/0.4	0.5/0.0	0.6/1.2	0.50/0.0	2.4/2.3	0.6/1.2		
15	RFA	AAV-DIO-eNpHr	3.3	3.4	0.6/1.2	3.4	1.4	0.6/1.2	RFA	N/A
	CFA	retroAAV-cre	0.2/-0.4	0.7-0.1	0.6/1.2	0.7/-.1	2.8/2.6	0.6/1.2		
16	RFA	AAV-DIO-eNpHr	3.4	3.6	0.6/1.2	3.6	1.6	0.6/1.2	RFA	CFA
	CFA	retroAAV-cre	0.4/-0.2	1.0/0.6	2.2/2.3	1.0/0.6	2.62.5	0.6/1.2		

Table S3: Injection coordinates, silicon probes, and optical fiber implantation location for inhibition experiments. Related to Figure 5.

Rat #	Injection area	Injection coordinates		
		AP (mm_)	ML (mm)	DV (mm)
19	RFA	+3.5	+/- 1.5	-1.2, -0.6
4	RFA	+3.5	+/- 1.5	-1.2, -0.6
5	RFA	+3.5	+/- 1.5	-1.2, -0.6
8	RFA	+3.5	+/- 1.5	-1.2, -0.6

Table S4: Injection coordinates for EM experiments. Related to Figure 4.